Suppression of the Methyl Radical Loss from Acetone Cation within $(CH_3COCH_3)_nCH_3COCH_3^+$ Clusters

Yonghoon Lee,* Myoung-Kyu Oh, Sung-Chul Choi, Do-Kyeong Ko, and Jongmin Lee

Advanced Photonics Research Institute, Gwangju Institute of Science and Technology, Gwangju 500-712, Korea
**E-mail: lyh@gist.ac.kr*
Received May 13, 2008

We have investigated the photophysics of the acetone radical cation in the vacuum ultraviolet energy region by multiphoton ionization combined with time-of-flight mass spectrometry in a cluster beam. We have found that the loss of methyl radical from the acetone radical cations is remarkably suppressed at 10.5 eV when they are solvated by a few neutral acetone molecules. The cluster ion mass spectra obtained by nanosecond and picosecond laser pulses reveal that there are intermolecular processes, occurring in several tens of picoseconds, which are responsible for the survival of the acetone cations in clusters. This remarkable solvation effect on the yield of the methyl radical loss from the acetone cation can be rationalized by the intracluster vibrational energy redistribution and the self-catalyzed enolization which compete with the methyl radical loss process.

Key Words : Acetone cation, Cluster, Multiphoton ionization, Mass spectrometry

Introduction

Study of molecular clusters bound by weak van der Waals forces or hydrogen bonding has provided a valuable microscopic understanding of physical and chemical properties of bulk condensed matter.[1,2] From the investigation of the clusters using laser spectroscopic methods, we can obtain an insight into chemical reactions and local structures in the bulk system such as solute-solvent interactions and hydrogen bonding structures. Particularly, combining mass spectrometry with laser spectroscopy for the investigation of molecular clusters formed in a supersonic jet, the properties of different cluster species can be easily distinguished. Therefore, this powerful methodology has filled the gap between gas-phase isolated molecules and bulk matter.

Acetone (C_3H_6O) is the simplest aliphatic ketone, which serves various chemical processes as an important solvent. In addition to being produced as a chemical through the cumene process, acetone is emitted from both biogenic and anthropogenic sources.[3,4] This volatile organic compound plays an important role in atmospheric chemistry as a source of hydroxyl radicals[3] and also in medical diagnosis as a disease marker for human diabetes.[5] The keto-enol tautomerism of acetone ($CH_3COCH_3 \leftrightarrow CH_3C(OH)CH_2$) is the famous representative of chemical equilibriums through intramolecular hydrogen shift. Acetone is ionized above 9.708 eV.[6] Appearance potential of the methyl radical loss from the acetone cation ($CH_3COCH_3^+ \rightarrow CH_3CO^+ + CH_3$) is 10.563 eV.[6] Recently, rich dissociation processes of the acetone cation in the vacuum ultraviolet (VUV) energy region have been investigated by threshold photoelectron photoion coincidence (TPEPICO) spectroscopy,[6] VUV photoabsorption and ionization using synchrotron radiation,[7,8] and electron impact ionization.[9] The dissociative ionization of acetone above the threshold energy of the methyl radical loss from the acetone cation was also observed in the previous multiphoton ionization (MPI) experiments.[10,11] For the acetone clusters, Tzeng *et al.* reported unimolecular decomposition of acetone cluster ions and the influence of water solvation on the intracluster dehydration reaction,[12] and Trott *et al.* reported the ionization potentials of $(CH_3COCH_3)_2$, $(CH_3COCH_3)_3$, and $(CH_3COCH_3)_4$, and the binding energy between the neutral and ionic species.[13] The enolization barrier energy of the acetone cation is 1.6 eV.[14] Trikoupis and Terlouw found that an appropriate base molecule can catalyze the enolization of the acetone cation.[15] Recently, it was experimentally observed that the neutral acetone molecule catalyzes the enolization of its radical cation by Fourier transform ion cyclotron resonance (FT-ICR) mass spectrometry[16] and collision-induced dissociation (CID) mass spectrometry with chemical ionization source.[17] Trikoupis *et al.* identified this catalyzed enolization by the parent neutral molecule as "self-catalysis" according to the definition of Clennan *et al.*[17,18] The self-catalyzed enolization of the acetone cation occurs via the proton transport catalysis from the aliphatic carbon to the carbonyl oxygen in the acetone cation.[17] In this mechanism, the proton affinity (PA) was found to be an important property of the catalyst. The intermediate value of PA between those at the aliphatic carbon and the carbonyl oxygen of the acetone cation is required for the efficient catalyst.[15]

In this work, we report the remarkable suppression of the methyl radical loss from the acetone cation solvated even by a single neutral acetone molecule in the vicinity of the threshold energy at 10.5 eV. Also, the cluster size effect on the yield of the methyl radical loss from the acetone cation has been observed. From the cluster ion mass spectra obtained by MPI using nanosecond and picosecond laser pulses combined with time-of-flight (TOF) mass spectrometric detection, we found that intermolecular processes are competing with the well-known methyl radical loss from the acetone cation in clusters. We suggest the intracluster vib-

rational energy redistribution (ICVR) and the self-catalyzed enolization as the competing intermolecular processes.

Experimental Section

Our experimental apparatus and techniques have been modified from those discussed previously.[19] Briefly, we prepared acetone cluster beams by expanding acetone vapor at room temperature with argon carrier gas (stagnation pressure 2.3 atm) through a pulsed valve (General valve series 9, 500-μm nozzle diameter). The pulsed jet was collimated by a skimmer with a 1.2-mm diameter, located at 5 cm away from the nozzle. The cluster beam and TOF chambers were differentially pumped by 10- and 6-inch diffusion pumps, respectively. In this controlled situation, we could generate acetone monomer and clusters consisting of 2-9 acetone molecules. The skimmed acetone cluster beam was intersected at right angles by an ionization laser at 8 cm away from the skimmer. The third and fourth harmonics of a nanosecond Nd:YAG laser (Quantel Brilliant b, ~8 ns) and the third harmonic of a picosecond Nd:YAG laser (EKSPLA PL2143A, ~30 ps) were used. The laser beam was focused by a plano-convex lens (f = 20 cm). The resulting ions were accelerated by a double electrostatic field and detected by a dual microchannel plate through a 70-cm long field-free region in a linear TOF mass spectrometer. The mass spectrum was recorded by an oscilloscope (LeCroy Waverunner 6051, 500 MHz). The data were averaged over 500 laser shots.

Results and Discussion

A. Overview of TOF spectra. Figure 1 shows the TOF mass spectra between m/e = 20 and 530, obtained by nanosecond laser pulses at (a) 355 nm and (b) 266 nm. As shown in both Figures 1a and 1b, the m/e 43 peak, corresponding to the acetyl cation (CH_3CO^+), is the most abundant and the m/e 58 peak, corresponding to the acetone cation, is very weak. This indicates that the loss of methyl radical from the acetone cation occurs very intensively. Previously, Majumder *et al.* observed multiphoton ionization and fragmentation of acetone at 355 nm using TOF mass spectrometry and suggested that 3-photon ionization at 355 nm (10.5 eV) produces vibrationally excited acetone cations which undergo fast dissociation of methyl radical.[10] In our TOF spectrum obtained by MPI at 355 nm, weak peaks between m/e 90 and 530 appear, which can be assigned as cluster ion species (see Fig. 1a). However, no mass peak corresponding to the cluster ion species was observed by MPI at 266 nm. The mass peaks corresponding to the acetone, acetyl, and methyl cations, solvated by neutral acetone molecules, are indicated by "■", "●", and "▲" in Figure 1a, respectively. "n" represents the number of solvent molecules. Note that the abundances of the peaks corresponding to the acetone and acetyl cations solvated by the same number of solvent molecules are comparable. This indicates that the yield of loss of methyl radical from the acetone cation is significantly reduced in clusters.

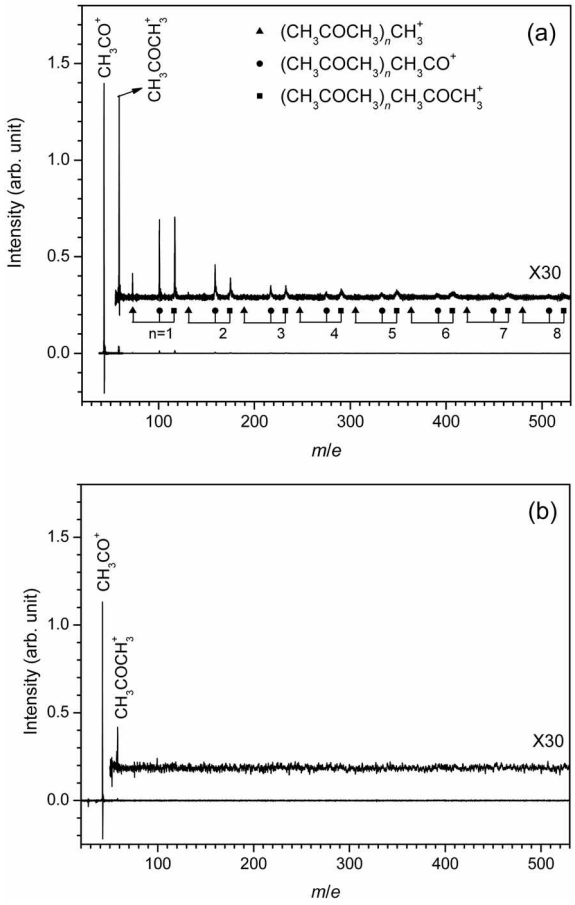

Figure 1. TOF mass spectra obtained by laser pulses at (a) 355 nm (b) 266 nm. In both cases, the laser pulse duration and power were ~8 ns and 10 mJ/pulse, respectively.

Figure 2 shows the laser power dependence of the m/e 43 peak by nanosecond laser pulses at 355 and 266 nm. The logarithms of the integrated intensities of the mass peaks

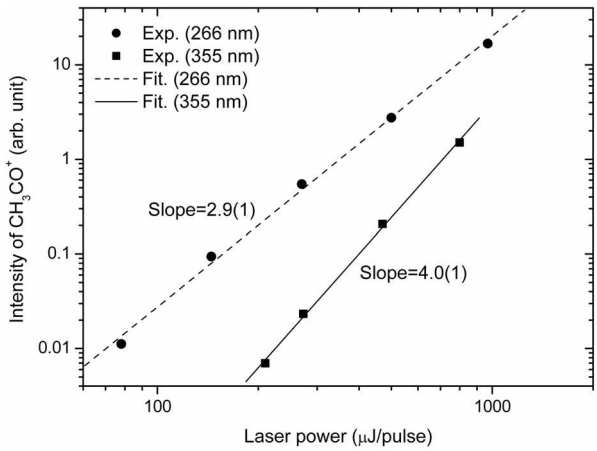

Figure 2. Laser power dependence of the m/e 43 peak corresponding to CH_3CO^+ in the TOF mass spectra obtained by 210, 273, 470, and 800 μJ/pulse at 355 nm, and 78, 145, 270, 500, and 970 μJ/pulse at 266 nm. The solid and dashed lines represent the linear fits of the logarithms of the measured data.

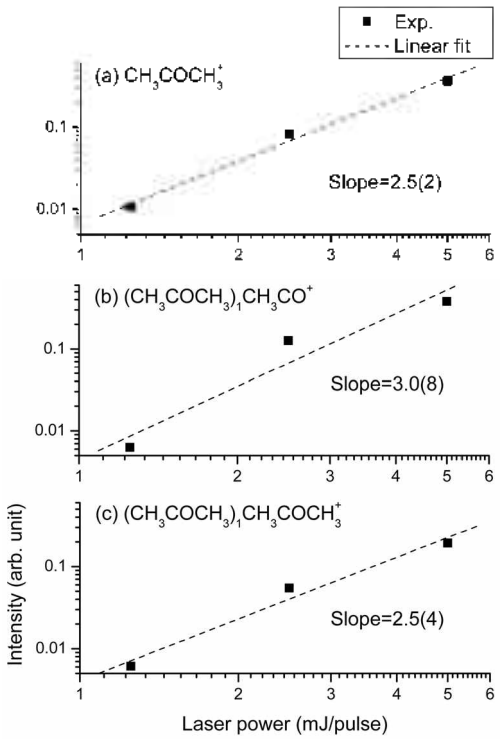

Figure 3. Laser power dependence of the *m/e* 58, 101, and 116 peaks corresponding to (a) $CH_3COCH_3^+$, (b) $(CH_3COCH_3)CH_3CO^+$, and (c) $(CH_3COCH_3)CH_3COCH_3^+$, respectively, in the TOF mass spectra obtained by 1.25, 2.5, and 5 mJ/pulse at 355 nm. The dashed lines represent the linear fits of the logarithms of the measured data.

were plotted with respect to the logarithms of the irradiated laser powers. These data were fitted to a linear function. Slopes of both linear fits were determined to be 4.0 (± 0.1) and 2.9 (± 0.1) for 355 nm and 266 nm, respectively. The numbers in parentheses are 1σ errors. From this analysis, the final ionic dissociative state is located at 14.0 eV, which corresponds to 4-photon energy at 355 nm and 3-photon energy at 266 nm. For MPI at 355 nm, the lower ionic energy level at 10.5 eV, populated by the 3-photon ionization at 355 nm, can also contribute to the mass spectrum of ionic species as observed in the previous experiment of Majumder *et al.*[10]

Figure 3 shows the laser power dependence of the mass peaks corresponding to (a) $CH_3COCH_3^+$ (*m/e* = 58), (b) $(CH_3COCH_3)CH_3CO^+$ (*m/e* = 101), and (c) (CH_3COCH_3)-$CH_3COCH_3^-$ (*m/e* = 116). The powers of 1.25, 2.5, and 5 mJ/pulse from the nanosecond laser at 355 nm were irradiated. The logarithms of the measured intensities were plotted with respect to the logarithms of the irradiated laser powers and fitted to a linear function. In each case, the slope of the linear fit indicates that the ions were produced by the 3-photon ionization at 355 nm. From this observation, we could find that the observed mass peak corresponding to bare acetone cation mainly came from the lower ionic energy level at 10.5 eV. This indicates that the yield of loss of methyl radical from the acetone cation at 14.0 eV is larger than that at 10.5 eV. Consistently, the intensity ratio of $[CH_3CO^-]/[CH_3COCH_3^-]$ observed by MPI at 266 nm is larger than that observed by MPI at 355 nm (compare the intensities of CH_3CO^+ and $CH_3COCH_3^+$ in Figs. 1a and 1b). More importantly, the laser power dependence of the mass peaks corresponding to $(CH_3COCH_3)CH_3CO^+$ and $(CH_3COCH_3)CH_3COCH_3^+$, shown in Figures 3b and 3c respectively, indicates that the observed cluster ionic species came from the ionic energy level at 10.5 eV, populated by 3-photon ionization at 355 nm.

The absence of the cluster ion mass peaks in the TOF spectrum obtained by MPI at 266 nm (see Fig. 1b) can be rationalized by the cluster disassembling. The large amount of excess energy deposited in the acetone cation by the absorption of 3 photons at 266 nm is, subsequently, redistributed into the intermolecular vibrational modes of the cluster. This is enough to disassemble the clusters. Trott et al. also reported the ionization potentials of acetone clusters (9.26 eV for $(CH_3COCH_3)_2$, 9.10 eV for $(CH_3COCH_3)_3$, and 9.02 eV for $(CH_3COCH_3)_4$ with the uncertainty of ± 0.03 eV) and the binding energy between the neutral and ionic species (0.538 eV).[13] Through 3-photon MPI at 355 nm, the cluster species can be populated in the lower ionic level at 10.5 eV. Taking account of the results (ionization potential of $(CH_3COCH_3)_2$ and binding energy between CH_3COCH_3 and $CH_3COCH_3^-$) in Ref. 13, we could find that the $(CH_3$-$COCH_3)CH_3COCH_3^-$ cluster can survive the disassembling into CH_3COCH_3 + $CH_3COCH_3^+$ by the deposition of 0.68 eV ($3h\nu$ at 355 nm – (ionization potential + binding energy)) into the vibrational modes of the acetone cations in the energy level at 10.5 eV. The 2-photon ionization process at 266 nm should be considered for the clusters. The 2-photon energy at 266 nm corresponds to 9.32 eV, which is slightly above the ionization potential of $(CH_3COCH_3)_2$ (9.26 eV). However, the contribution of the 2-photon MPI at 266 nm to the cluster ionization was not observed although the excess energy above the ionization potential (0.06 eV) was smaller than the binding energy between CH_3COCH_3 and $CH_3COCH_2^-$. This is, probably, due to the very low photoionization efficiency of the clusters just above their ionization potentials, which might not be enough to be detected in our experiment. According to the photoionization yield spectra of the acetone clusters, $(CH_3COCH_3)_2$, $(CH_3COCH_3)_3$, and $(CH_3COCH_3)_4$, in Ref. 13, the ionization efficiency of the clusters grows very slowly from the ionization potential. Differently, the ionization efficiency of bare acetone shows the vertical increase across the ionization potential.

B. Solvation effect. Note that the mass peak corresponding to the acetyl cation fragment is not so much abundant in clusters as that in the isolated species (see Fig. 1a). The comparable intensities of the acetyl fragment and acetone cations, solvated by a few neutral acetone molecules, indicate that the loss of methyl radical from the acetone cation is remarkably suppressed even by attaching a single neutral acetone solvent molecule. More interestingly, we can find the clear cluster size effect on the yield of loss of methyl radical. Figure 4 shows (a) the normalized intensities of the mass peaks corresponding to $(CH_3COCH_3)_nCH_3CO^-$ and

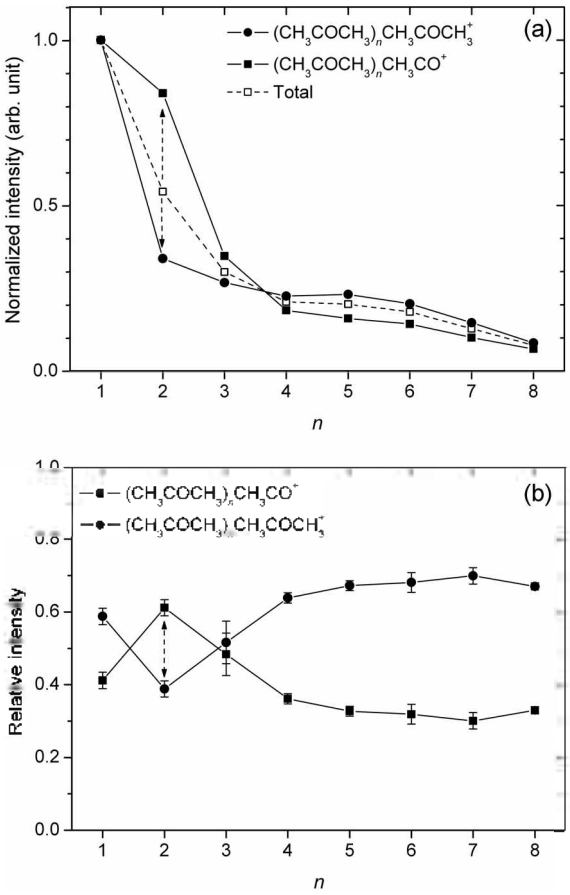

Figure 4. (a) Normalized intensities of $(CH_3COCH_3)_nCH_3CO^+$, $(CH_3COCH_3)_nCH_3COCH_3^+$, and their sum with respect to the intensity values at n = 1. (b) The intensity ratios of $[(CH_3COCH_3)_nCH_3CO^+]/\{[(CH_3COCH_3)_nCH_3CO^+] + [(CH_3COCH_3)_nCH_3COCH_3^+]\}$ and $[(CH_3COCH_3)_nCH_3COCH_3^+]/\{[(CH_3COCH_3)_nCH_3CO^+] + [(CH_3COCH_3)_nCH_3COCH_3^+]\}$. The vertical arrows in (a) and (b) indicate the cluster size effect on the yield of loss of methyl radical from the acetone cation.

$(CH_3COCH_3)_nCH_3COCH_3^+$, and their sum with respect to the intensities at n = 1, and (b) the intensity ratios of $[(CH_3COCH_3)_nCH_3CO^+] / \{[(CH_3COCH_3)_nCH_3CO^+] + [(CH_3COCH_3)_nCH_3COCH_3^+]\}$ and $[(CH_3COCH_3)_nCH_3CO\text{-}CH_3^+] / \{[(CH_3COCH_3)_nCH_3CO^+] + [(CH_3COCH_3)_nCH_3CO\text{-}CH_3^+]\}$. In the case of n = 2, the intensity of $(CH_3COCH_3)_2\text{-}CH_3CO^+$ is particularly strong and clearly correlated with the decrease in the intensity of $(CH_3COCH_3)_2CH_3COCH_3^+$, as indicated by the arrows in Figures 4a and 4b. Also, the similar correlation between the intensities of the mass peaks corresponding to $(CH_3COCH_3)_3CH_3CO^+$ and $(CH_3COCH_3)_3\text{-}CH_3COCH_3^+$ is found. This correlation between the intensities of the acetone and acetyl fragment cations, solvated by the same number of neutral acetone molecules, also confirms that the solvated acetone cation is the parent species of the solvated acetyl cation. We summarize these observations as follows:

(i) The loss of methyl radical from the acetone cations is greatly suppressed even by a single solvent molecule (n = 1).

(ii) The solvation effect suppressing the loss of methyl radical becomes slightly weaker upon the addition of one more solvent molecule (n = 1 → 2).

(iii) As the number of solvent molecules increases further (n = 2 → 3, 4, 5, ...). the solvation effect suppressing the loss of methyl radical recovers.

Particularly, the "cluster size effect" refers to the above observations (ii) and (iii).

C. Competing processes with the methyl radical loss. The solvated acetone cations are populated in the ionic energy level at 10.5 eV by MPI at 355 nm. The appearance potential for the loss of methyl radical from the acetone cation solvated by a neutral acetone molecule, $(CH_3CO\text{-}CH_3)_2 \rightarrow (CH_3COCH_3)CH_3CO^+ + CH_3 + e^-$, was previously reported as 10.08 eV with the uncertainty of ± 0.05 eV.[13] The ionic energy level is very close to this dissociation threshold energy in the cluster. Therefore, through ICVR relaxing the energy of 0.4 eV from the hot acetone cation to the intermolecular vibrational modes of the cluster, the solvated acetone cation can survive the loss of methyl radical. Generally, the intramolecular or intracluster vibrational energy redistributions occur in several tens of picoseconds or shorter.[20] Figure 5 compares the TOF mass spectra obtained by nanosecond and picosecond laser pulses at 355 nm. When the shorter laser pulse is irradiated, the yield of loss of methyl radical increases twice approximately. This comparison reveals that there are the intermolecular processes, which occur in several tens of picoseconds and are responsible for the suppression of the methyl radical loss in clusters. The pulse duration of the picosecond laser (30 ps) is not so much enough for the relaxation processes.

However, the redistribution of the excess energy through ICVR process can not explain the cluster size effect on the yield of loss of methyl radical in the n = 2 cluster (indicated by arrows in Figs. 4a and 4b). Another process which acetone cations undergo in this VUV energy region is the enolization. As previously reported by the collision-type experiments, a neutral acetone molecule catalyzes the enolization of the acetone cation.[15-17] Clusters provide ideal

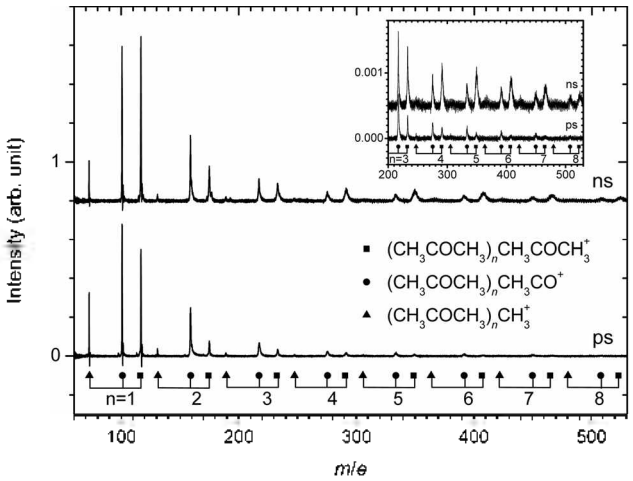

Figure 5. TOF mass spectra obtained by nanosecond (Δt ~ 8 ns) and picosecond (Δt ~ 30 ps) laser pulses at 355 nm. The inset shows the expanded spectra between m/e = 200 and 530.

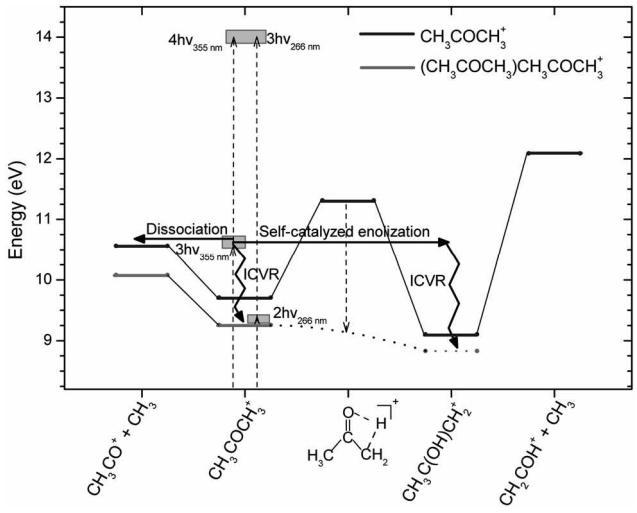

Figure 6. Energy level diagrams of the bare acetone keto and enol cations and the mono-solvated acetone cation, (CH_3COCH_3)-$CH_3COCH_3^+$. Vertical dashed lines represent the multiphoton ionization pathways at 355 and 266 nm and the stabilization of the barrier energy from keto to enol cations. Experimental data for the bare acetone keto and enol cations were taken from Refs 6, 14, and 23. Experimental data for $(CH_3COCH_3)CH_3CO^+ + CH_3$ and $(CH_3COCH_3)CH_3COCH_2^+$ were taken from Ref. 13. The energy level of $(CH_3COCH_3)CH_3C(OH)CH_2^+$ was located 0.43 eV below that of $(CH_3COCH_3)CH_3COCH_3^+$ based on the theoretical prediction in Ref. 17. The energy level of the transition state in the cluster is not available currently. Thus, the energy level, represented by the horizontal dotted line, just indicates that the enolization process is available in the cluster at 10.5 eV. The solid arrows indicate the dynamic processes occurring in the vicinity of the threshold energy of loss of methyl radical, which are discussed in text.

environment for the enolization of acetone cations. In clusters, collisions between a reactant and a catalyst for the enolization are not necessary. The enolization of the acetone cation is catalyzed instantly by an intact neutral acetone molecule. The enolization is also followed by ICVR. The energy of the hot enol cations flows to the intermolecular vibrational modes of the cluster. The enol cation thus relaxes into its potential minimum. Trikoupis *et al.* reported that the barrier for the catalyzed enolization lie below the energy of the separated starting species, $CH_3COCH_3 + CH_3COCH_3^+$, based on their experimental and theoretical results.[17]

The cluster size effect can come from the influence of the cluster binding on the PA values of the acetone cation and the catalyzing neutral acetone molecule.[15] The PA values of the acetone cation at the aliphatic carbon site (PA_C^{cation}) and at the carbonyl carbon site (PA_O^{cation}) were determined to be 185.5 and 195.0 kcal/mol, respectively, by FT-ICR mass spectrometry[16] and that of the neutral acetone ($PA_O^{neutral}$) was determined to be 194.1 kcal/mol.[21] The balanced PA values of the reactant and catalyst (PA_C^{cation} (185.5 kcal/mol) < $PA_O^{catalyst}$ (194.1 kcal/mol) < PA_O^{cation} (195.0 kcal/mol)) for the efficient catalyzed enolization are found to be sensitively influenced by clustering. Hu *et al.* reported the PA values of neutral acetone and its clusters of ring-like stable structures by ab initio quantum chemical computation.[22] According to their calculation, PA of neutral acetone clusters is increased by binding of additional neutral acetone molecules. Also, the increase in PA (15%) from monomer (209.2 kcal/mol) to dimer (241.7 kcal/mol) is substantially larger than those by the subsequent binding upto heptamer (2.2-0.3%). Based on this theoretical prediction, we could find that binding of an additional neutral acetone molecule to $(CH_3COCH_3)CH_3$-$COCH_3^+$ would most significantly throw the PA values out of balance. The additional neutral acetone molecule can bind to either the catalyst, CH_3COCH_3 or the acetone cation. In the former case, the PA value of the catalyst is increased significantly upon this addition of the second neutral acetone molecule. Thus the balanced PA values ($PA_C^{cation} < PA_O^{catalyst} < PA_O^{cation}$) are changed into $PA_C^{cation} < PA_O^{cation} < PA_O^{catalyst}$. This reduces the efficiency of the catalyzed enolization of acetone cations. Upon the subsequent binding of neutral acetone molecules to the catalyst, the PA value of the catalyst would increase further and, however, become saturated. Probably, binding of neutral acetone molecules to the acetone cation has the similar effect on PA_O^{cation}. In most clusters, both the acetone cation and catalyst would interact with at least one solvent molecule. In these clusters, the balance of PA values for the efficient catalysis would not be perturbed much since PA_O^{cation} and $PA_O^{catalyst}$ behaves similarly. Therefore, the efficiency of enolization in most clusters would be similar to that in $(CH_3COCH_3)CH_3CO$-CH_3^+. For the cluster structures, in which the solvent molecules exclusively bind to either the catalyst or the acetone cation, the efficiency of the enolization would be lower than that of $(CH_3COCH_3)CH_3COCH_3^-$. The contribution of this type of the cluster structure is largest for $n = 2$. This may lead to the observed cluster size effect on the yield of loss of methyl radical from the acetone cation. The particularly inefficient enolization of the acetone cation in the cluster of $n = 2$ results in the relatively more intensive loss of methyl radical. Figure 6 shows the schematic energy level diagrams of the bare acetone cation and the cluster of $n = 1$ which is a representative of clusters.

Conclusion

We have observed the remarkable suppression of the loss of methyl radical from the acetone cation in clusters. The ICVR process has been found to play an important role in the dynamics of the acetone cation in clusters near the threshold energy of the methyl radical loss. The ICVR competes with the well-known methyl radical loss process with the consequence that the yield of loss of methyl radical from the acetone cation is reduced in clusters. Furthermore, the cluster size effect on the yield of the methyl radical loss can be rationalized by employing another dynamic process, enolization, which becomes available through the self-catalysis in clusters. The suggested ICVR and self-catalyzed enolization processes works exclusively in clusters, in which solvent molecules both provide bath modes for ICVR and act as the catalyst for the enolization of the acetone cation. This study encourages the spectroscopic study on the enol cation produced in the clusters such as the size-selected

infrared photodissociation spectroscopy, which can show the self-catalyzed enolization more clearly and provide the detailed information on the cluster structure.

Acknowledgments. This work was supported by MEST (Ministry of Education, Science and Technology) of Korea through APRI-Research Program of GIST. The authors thank Dr. Joon Heon Kim for technical support for using the picosecond laser equipment.

References

1. Cheng, P.-Y.; Baskin, J. S.; Zewail, A. H. *PNAS* **2006**, *103*, 10570.
2. Ahn, D.-S.; Lee, S. *Bull. Korean Chem. Soc.* **2007**, *28*, 725.
3. Holzinger, R.; Lee, A.; Paw, K. T.; Goldstein, A. H. *Atmos. Chem. Phys.* **2005**, *5*, 67.
4. Szopa, S.; Aumont, B.; Madronich, S. *Atmos. Chem. Phys.* **2005**, *5*, 2519.
5. Marczin, N.; Kharitonov, S. A.; Yacoub, S. M. H.; Barnes, P. J. *Disease Markers in Exhaled Breath*; Marcel Dekker: New York, 2003.
6. Fogleman, E. A.; Koizumi, H.; Kercher, J. P.; Sztáray, B.; Baer, T. *J. Phys. Chem. A* **2004**, *108*, 5288.
7. Nobre, M.; Fernandes, A.; Ferreira da Silva, F.; Antunes, R.; Almeida, D.; Kokhan, V.; Hoffmann, S. V.; Mason, N. J.; Eden, S.; Limão-Vieira, P. *Phys. Chem. Chem. Phys.* **2008**, *10*, 550.
8. Wei, L.; Yang, B.; Yang, R.; Huang, C.; Wang, J.; Shan, X.; Sheng, L.; Zhang, Y.; Qi, F. *J. Phys. Chem. A* **2005**, *109*, 4231.
9. Vacher, J. R.; Jorand, F.; Blin-Simiand, N.; Pasquiers, S. *Int. J. Mass Spectrom.* **2008**, *273*, 117.
10. Majumder, C.; Jayakumar, O. D.; Vatsa, R. K.; Kulshreshtha, S. K.; Mittal, J. P. *Chem. Phys. Lett.* **1999**, *304*, 51.
11. Zhu, Y. F.; Allman, S. L.; Phillips, R. C.; Garrett, W. R.; Chen, C. H. *Chem. Phys.* **1996**, *202*, 175.
12. Tzeng, W. B.; Wei, S.; Castleman, A. W., Jr. *J. Am. Chem. Soc.* **1989**, *111*, 6035.
13. Trott, W. M.; Blais, N. C.; Walters, E. A. *J. Chem. Phys.* **1978**, *69*, 3150.
14. (a) Williams, D. H. *Acc. Chem. Res.* **1977**, *10*, 286. (b) Burgers, P. C.; Holmes, J. L. *Org. Mass Spectrom.* **1982**, *17*, 123.
15. Trikoupis, M. A.; Terlouw, J. K. *J. Am. Chem. Soc.* **1998**, *120*, 12131.
16. Mourgues, P.; Chamot-Rooke, J.; van der Rest, G.; Nedev, H.; Audier, H. E.; McMahon, T. B. *Int. J. Mass Spectrom.* **2001**, *210/211*, 429.
17. Trikoupis, M. A.; Burgers, P. C.; Ruttink, P. J. A.; Terlouw, J. K. *Int. J. Mass Spectrom.* **2002**, *217*, 97.
18. Clennan, E. L.; Dobrowolski, P.; Greer, A. *J. Am. Chem. Soc.* **1995**, *117*, 9800.
19. Lee, Y.; Yoon, Y.; Baek, S. J.; Joo, D.-L.; Ryu, J.-s.; Kim, B. *J. Chem. Phys.* **2000**, *113*, 2116.
20. Yamada, Y.; Katsumoto, Y.; Ebata, T. *Phys. Chem. Chem. Phys.* **2007**, *9*, 1170.
21. Hunter, E. P. L.; Lias, S. G. *J. Phys. Chem. Ref. Data* **1998**, *27*, 413.
22. Hu, Z.; Jin, M.-x.; Xu, X.-s.; Cheng, X.-h.; Ding, D.-j. *Front. Phys. China* **2006**, *3*, 275.
23. Lias, S.; Bartmess, J. E.; Liebman, J. F.; Holmes, J. L.; Levin, R. D.; Mallard, W. G. *J. Phys. Chem. Ref. Data* **1988**, *17*, Supplement 1.